Electroencephalogram signatures of ketamine anesthesia-induced unconsciousness

Citation: Akeju, Oluwaseun, et al. “Electroencephalogram Signatures of Ketamine Anesthesia-Induced Unconsciousness.” Clinical Neurophysiology 127, 6 (June 2016): 2414–2422 © 2016 International Federation of Clinical Neurophysiology

Published Version: http://dx.doi.org/10.1016/J.CLINPH.2016.03.005

Publisher: Elsevier

Permanent Link: http://hdl.handle.net/1721.1/112233

Version: Author's final manuscript: final author’s manuscript post peer review, without publisher’s formatting or copy editing

HHS Public Access

Author manuscript

Clin Neurophysiol. Author manuscript; available in PMC 2017 June 01.

Published in final edited form as:

Clin Neurophysiol. 2016 June ; 127(6): 2414–2422. doi:10.1016/j.clinph.2016.03.005.

Electroencephalogram Signatures of Ketamine-Induced Unconsciousness

Oluwaseun Akeju[1,2], **Andrew H. Song**[3], **Allison E. Hamilos**[2,4,5], **Kara J. Pavone**[1], **Francisco J. Flores**[1,2,3], **Emery N. Brown**[1,2,3,4,5], and **Patrick L. Purdon**[1,2,3]

[1]Department of Anesthesia, Critical Care and Pain Medicine, Massachusetts General Hospital, Boston, MA, USA

[2]Harvard Medical School, Boston, MA, USA

[3]Department of Brain and Cognitive Science, Massachusetts Institute of Technology, Cambridge, MA, USA

[4]Harvard-Massachusetts Institute of Technology Division of Health Sciences and Technology, Massachusetts Institute of Technology, Cambridge, MA, USA

[5]Institute for Medical Engineering and Sciences, Massachusetts Institute of Technology, Cambridge, MA, USA

Abstract

Objectives—Ketamine is an N-methyl-D-aspartate receptor antagonist commonly administered as a general anesthetic. However, circuit level mechanisms to explain ketamine-induced unconsciousness in humans are yet to be clearly defined. Disruption of frontal-parietal network connectivity has been proposed as a mechanism to explain this brain state. However, this mechanism was recently demonstrated at subanesthetic doses of ketamine in awake-patients. Therefore we investigated whether there is an electroencephalogram (EEG) marker for ketamine-induced unconsciousness.

Methods—We retrospectively studied the EEG in 12 patients who received ketamine for the induction of general anesthesia. We analyzed the EEG dynamics using power spectral and coherence methods.

Results—Following the administration of a bolus dose of ketamine to induce unconsciousness, we observed a “gamma burst” EEG pattern that consisted of alternating slow-delta (0.1-4 Hz) and

Corresponding Author: Oluwaseun Akeju, 55 Fruit Street, Jackson Building, Rm. 460, Boston, MA 02114, USA, Tel.: +1-617-724-7200, oluwaseun.akeju@mgh.harvard.edu.

Conflict of interest

The authors Oluwaseun Akeju, Emery N. Brown, and Patrick L. Purdon have submitted a provisional patent application describing the use of the EEG measures described in this manuscript for monitoring sedation and general anesthesia. All other authors declare no competing interests.

gamma (~27-40 Hz) oscillations. This pattern was also associated with increased theta oscillations (~4-8 Hz) and decreased alpha/beta oscillations (~10-24 Hz).

Conclusions—Ketamine-induced unconsciousness is associated with a gamma burst EEG pattern.

Significance—We postulate that the gamma burst pattern is a thalamocortical rhythm based on insights previously obtained from cat neurophysiological experiments. This EEG signature of ketamine-induced unconsciousness may offer new insights into general anesthesia induced brain states.

Keywords

EEG; unconsciousness; ketamine; anesthesia; slow oscillations; gamma oscillations

Introduction

Ketamine is an N-methyl-D-aspartate (NMDA) receptor antagonist that is used as a dissociative anesthetic (Domino et al. , 1965, Corssen et al. , 1966), a research model for schizophrenia (Insel, 2010), and a fast acting treatment for major depressive disorder (Zarate et al. , 2006). At low doses, ketamine produces a dissociative state characterized by hallucinations, altered sensory perception and analgesia, while at higher doses it induces a state of unconsciousness appropriate for general anesthesia. For instance, an intravenous induction dose of ketamine (1-2mg/kg) causes a rapid loss of consciousness that typically lasts for approximately 10 minutes (White et al. , 1985, Vuyk et al. , 2015). The use of ketamine as a general anesthetic in clinical practice is commonplace. For instance, during the recent propofol drug shortage in the United States, ketamine was one of the few alternative agents available for the induction of general anesthesia. However, we do not yet understand the circuit level mechanisms to explain ketamine-induced unconsciousness, and lack principled neurophysiological signatures that could be used to monitor the brain during ketamine-induced unconsciousness.

At the receptor level, ketamine blocks excitatory NMDA receptors on fast-spiking cortical interneurons more effectively than those on pyramidal neurons. This results in down regulation of inter-neuron activity, and decreased GABA release at the interneuron-pyramidal neuron synapse (Homayoun et al. , 2007, Seamans, 2008). This decrease in inhibitory tone (decreased GABA release) results in markedly excited pyramidal neurons. This explains why ketamine is associated with increased cerebral glucose utilization and blood flow (Langsjo et al. , 2004, Langsjo et al. , 2005), and increased EEG gamma oscillations (Ferrer-Allado et al. , 1973, Schwartz et al. , 1974, Schultz et al. , 1990, Engelhardt et al. , 1994, Hering et al. , 1994, Lee et al. , 2013, Blain-Moraes et al. , 2014). Thus, the neurophysiological profile observed during ketamine-induced unconsciousness, which is suggestive of an active brain, is perplexing and remains a subject of intense interest in neuroscience.

Induction and maintenance of general anesthesia is associated with morbidity and mortality risks (Arbous et al. , 2005, Cottrell, 2008). Therefore, human volunteer research studies of

ketamine at general anesthesia levels are limited and challenging. However, an emerging paradigm to understand better the mechanisms of anesthetic action is to study electroencephalogram (EEG) recordings obtained during routine clinical care, and relate neurophysiological findings to the behavioral state encountered, and known neural circuit level mechanisms. We have found this approach an effective means to provide key insights into the mechanisms of anesthetic ac(Akeju et al. , 2014, Purdon et al. , 2015a, Pavone et al. , 2016).

Therefore, we retrospectively studied the EEG (n=12) during unconsciousness induced by ketamine using spectral and coherence analysis methods. We report that ketamine-induced unconsciousness defined by the behavioral state of unresponsiveness to verbal and tactile stimuli is associated with a characteristic gamma burst pattern (slow oscillations alternating with gamma oscillations), and we relate this pattern to cat neurophysiological experiments to suggest that the gamma burst pattern is a thalamocortical rhythm.

Materials and Methods

Patient Selection and Data Collection

The Human Research Committee at Massachusetts General Hospital approved this retrospective observational study. We reviewed our database of general anesthesia and simultaneous EEG recordings collected between September 1, 2011 and December 1, 2015. We identified 12 cases with baseline EEG recordings and ketamine (10 mg/mL; Bioniche Pharma, Lake Forest, IL) administration as the sole hypnotic agent for induction of general anesthesia. The EEGs of the 12 subjects were each reviewed for spectral artifacts and noise, and based on chart review, none of the patients had neurological or psychiatric abnormalities that could have interfered with the EEG.

Frontal EEG data were recorded using the Sedline brain function monitor (Masimo Corporation, Irvine, CA). The EEG data were recorded with a pre-amplifier bandwidth of 0.5 to 92 Hz, sampling rate of 250 Hz, with 16-bit, 29 nV resolution. The standard Sedline Sedtrace electrode array records from electrodes located approximately at positions Fp1, Fp2, F7, and F8, with ground electrode at Fpz and reference electrode approximately 1 cm above Fpz. Electrode impedance was less than 5k in each channel.

For all 12 patients, we selected EEG data segments by matching information from the electronic anesthesia record (Metavision, Dedham, MA) to the EEG and further confirmed the match by EEG analysis in the spectral domain (i.e. onset of anesthetic vapor on the electronic anesthesia record was manifest on the EEG by large power in slow, alpha and beta frequency bands). The electronic medical record was used to confirm ketamine as the sole hypnotic agent administered (isoflurane, sevoflurane, desflurane and nitrous oxide were not co-administered). Prior to the induction of general anesthesia with a bolus dose of ketamine, (n=8; mean ± standard deviation; 1.8± 0.5 mg) and/or fentanyl (n=9; 183 ± 79 mcg) were administered for anxiolysis and to block the sympathetic response to laryngoscopy, respectively. General anesthesia was induced with ketamine (mean ± standard deviation; 176 ± 32 mg) and intubation was carried out using succinylcholine, cisatracurium, or rocuronium for muscle relaxation. The gamma burst epochs were obtained 131 ± 86 seconds after the

induction of general anesthesia, while the beta/gamma stable epochs were obtained 467 ± 106 seconds after the induction of general anesthesia. We defined gamma burst as gamma-oscillations that were interrupted by slow-delta oscillations, and beta/gamma stable as beta/gamma oscillations that were not interrupted by slow-delta oscillations. Given the doses of ketamine administered, and the underlying pharmacokinetic and pharmacodynamic properties of ketamine (Vuyk et al. , 2015), we infer that the plasma levels of ketamine during the gamma burst were at therapeutic levels for unconsciousness, while the plasma levels of ketamine during the beta/gamma stable pattern were transitioning from therapeutic to sub-anesthetic levels.

Table 1 summarizes the patient characteristics and co-administered medications. Immediately prior to muscle relaxation and airway instrumentation, the patients (n=12) did not respond to both verbal commands and lash reflex. During this period, the EEG was noted to be in the gamma burst pattern by time domain visualization. For all epochs analyzed, general anesthesia was maintained by the induction dose of ketamine previously administered. That is, no other anesthetics were administered during the gamma burst and beta/gamma stable epochs. Muscle relaxation was maintained with cisatracurium or rocuronium, and none of the patients in our study cohort experienced post-operative recall.

Spectral Analysis

For each patient, we computed the power spectrum and spectrogram using multitaper spectral methods implemented in the Chronux toolbox (Percival et al. , 1993). To obtain estimates of power spectra that are robust to noise and artifacts, we derived an EEG electrode that equally weighted the signals obtained from Fp1, Fp2, F7 and F8 (average of all four channels). The parameters for the multitaper spectral analysis were: window length T = 2s with no overlap, time-bandwidth product TW = 3, number of tapers K = 5, and spectral resolution of 3 Hz. We also computed group-level spectrograms by taking the median across all patients. We did not normalize the EEG power, rather we computed the absolute power. We calculated the median spectra and 95% confidence intervals using a bootstrap procedure. Bootstrap samples for the spectrum were drawn from the full sample of data, consisting of 60 non-overlapping 2-second EEG windows for each subject. We computed the median spectrum across subjects and repeated this procedure 10,000 times to obtain bootstrapped spectral estimates of the median.

Coherence Analysis

The coherence $C_{xy}(f)$ between two signals x and y is defined as

$$C_{xy}(f) = \frac{|S_{xy}(f)|}{\sqrt{S_{xx}(f)\,S_{yy}(f)}}$$

where $S_{xy}(f)$ is the cross-spectrum between the signals $x(t)$ and $y(t)$, $S_{xx}(f)$ is the power spectrum of the signal $x(t)$ and $S_{yy}(f)$ is the power spectrum of the signal $y(t)$. The coherence can be interpreted as a frequency-dependent correlation coefficient, and also as a measure of association between two signals at the same frequency. The coherogram is a time-varying

version of the coherence, estimated using consecutive windows of EEG data. We estimated the coherence between the two distant frontal EEG electrodes FP1-F7 and FP2-F8 for each patient using multitaper methods and cohgramc function implemented in the Chronux toolbox (Percival et al. , 1993). The parameters for the multitaper coherence analysis, and methods for calculating the group-level coherograms and median coherence were the same as those outlined for spectral analysis.

Statistical Analysis

To assess statistical significance for the difference in spectra and coherence at each frequency, we computed the 95% confidence interval of the median difference between groups by using an empirical bootstrap approach. We resampled spectral and coherence estimates for each non-overlapping window to obtain replicates of the estimates for each subject and took the median value across subjects for each group. We took the difference between two median estimates, repeated this 10,000 times and calculated the 95% confidence interval of the median difference at each frequency. To account for the underlying spectral resolution of the spectral and coherence estimates, we considered differences to be significant only if they are present for contiguous frequencies over a frequency band wider than the spectral resolution, 2W.

Results

Spectral analysis

Gamma Burst versus Baseline Power Spectra—Immediately after the induction of general anesthesia, we observed a “gamma burst” pattern (n = 12), consisting of gamma oscillations alternating with slow oscillations (Fig. 1), that eventually transitioned to a “beta/gamma stable” pattern in all of the subjects (n = 11). Figure 2 is an illustrative spectrogram showing the evolution of the gamma burst pattern after an induction dose of ketamine. The gamma burst EEG pattern was evident in all patients studied. We computed group level spectrograms (Fig. 3) and found that compared with baseline, gamma burst exhibited increased power in the slow, delta, theta and gamma frequency ranges (Fig. 3A,B). To describe these differences, we compared the spectra during gamma burst to baseline spectra and found significant differences in power (Fig. 4A,B; gamma burst > baseline, 0.1-8.3 Hz, 26.9-50 Hz; gamma burst < baseline, 10.3-24.4 Hz;). The peak median difference (gamma burst – baseline) in slow-delta power (power difference [95% confidence interval]) was 6.9 dB [4.8 dB, 9 dB] at 0.5 Hz. The peak median difference in theta power was 4.6 dB [3.6 dB, 5.7 dB] at 4.4 Hz. The peak median difference in beta power was −3.5 dB [−4.3 dB, −2.7 dB] at 18.5 Hz. The peak median difference in gamma power was 7.5 dB [5.7 dB, 9.4 dB] at 39.1 Hz. Thus, the largest changes occurred in the slow-delta and gamma frequency bands.

Beta/gamma stable versus Baseline Power Spectra—Compared to baseline, we observed differences in the raw EEG and spectrograms during the beta/gamma stable pattern. The spectrogram during the beta/gamma stable pattern exhibited increased power in theta and gamma frequency bands (Fig. 3A,C). To describe these differences, we compared the spectra during beta/gamma stable to baseline spectra and found significant differences in power (Fig. 4C,D; beta/gamma stable > baseline, 0.1-7.8 Hz, 31.25-40.5 Hz; gamma burst <

baseline, 9.2-26.9 Hz, 44.9-48.3 Hz). The peak median difference (beta/gamma stable – baseline) in slow-delta power was 3.9 dB [3 dB, 4.9 dB] at 3.9 Hz. The peak median difference in theta power was 5.4 dB [4.4 dB, 6.4 dB] at 4.4 Hz. The peak median difference in beta power was −5.7 dB [−6.5 dB, −4.7 dB] at 18.1 Hz. The peak median difference in gamma power was 1.8 dB [0.7 dB, 2.8 dB] at 39.5 Hz. Thus, there was a further decrease in beta power with decreasing ketamine plasma levels necessary to maintain unconsciousness.

Ketamine Gamma Burst versus Beta/gamma stable Power Spectra—Compared to gamma burst, we observed differences in the raw EEG and spectrograms during the beta/gamma stable pattern. The spectrogram during the beta/gamma stable pattern exhibited decreased power in the slow and gamma frequency bands (Fig. 3B,C). To describe these differences, we compared the spectra during gamma burst to beta/gamma stable and found significant differences in power (Fig. 4E,F; beta/gamma stable < gamma burst, 0.1-3.4 Hz, 16.1-50 Hz). The peak median difference (beta/gamma stable – gamma burst) in slow-delta power was −5.2 dB [−7.3 dB, −3.1 dB] at 0.5 Hz. The peak median difference in beta power was −1.8 dB [−2.7 dB, −0.9 dB] at 15.6 Hz. The peak median difference in gamma power was −7.9 dB [−4.7 dB, −6.3 dB] at 41.5 Hz. Thus, as ketamine plasma levels decreased in the transition from burst to beta/gamma stable patterns, so too did EEG power within the slow-delta, beta, and gamma bands, suggesting a dose-response relationship. The largest changes occurred within the slow-delta and gamma bands.

Coherence analysis

Gamma Burst versus Baseline Coherence—Compared to baseline, we observed coherent gamma oscillations in the coherogram during gamma burst (Fig. 5). To describe these differences, we compared the coherence during gamma burst to baseline and found significant increases in coherence (Fig. 6A,B; gamma burst > baseline, 27.9-48.9 Hz). The peak median gamma coherence difference was at 38.6 Hz.

Beta/gamma stable versus Baseline Coherence—Compared to baseline, we also observed coherent gamma oscillations in the coherogram during beta/gamma stable (Fig. 5). To describe these differences, we compared the coherence during beta/gamma stable to baseline and found significant increases in coherence (Fig. 6C,D; beta/gamma stable > baseline, 25.4–28.3 Hz, 30.8–45.5 Hz). The peak median gamma coherence difference was at 38.6 Hz.

Gamma Burst versus Beta/gamma stable—We found that the beta/gamma stable and gamma burst group coherograms exhibited similar pattern of increased coherence in theta and gamma frequency bands (Fig. 5). When we examined the coherence structure of these periods, we did not find significant differences in coherence (Fig. 6E,F).

Discussion

Disruption of frontal-parietal network connectivity was recently proposed to explain ketamine-induced unconsciousness (Lee et al. , 2013, Blain-Moraes et al. , 2014). However, more recently, disruption of frontal-parietal network connectivity was demonstrated at subanesthetic doses of ketamine in awake-patients (Muthukumaraswamy et al. , 2015). This

mechanism has been postulated instead to explain the rapid anti-depressant effect of ketamine (Muthukumaraswamy et al. , 2015). This discrepancy highlights the need to understand in greater detail the underlying neurophysiological dynamics associated with ketamine-induced unconsciousness.

Ketamine is commonly associated with increased gamma oscillations in humans (Akeju et al. , 2015, Purdon et al. , 2015b). Our findings reveal novel oscillatory EEG dynamics, namely the gamma burst pattern, and its transition into a beta/gamma stable pattern, that occur during ketamine-induced unconsciousness. Following an intravenous induction dose of ketamine (1-2mg/kg), loss of consciousness is rapidly achieved (White et al. , 1985, Vuyk et al. , 2015). During this state, patients are not responsive to commands or painful stimuli, and by definition are in a general-anesthetic state. Therapeutic plasma ketamine levels, and the behavioral state of unconsciousness typically lasts for approximately 10 minutes, followed by a dissociative brain-state that may persist for hours (White et al. , 1985, Vuyk et al. , 2015). These findings may relate to the circuit level mechanism of the behavioral state that is induced by this drug at surgical anesthesia levels.

Slow Oscillations during Ketamine-Induced Unconsciousness

It has been hypothesized that the removal of substantial subcortical excitatory inputs to the cortex is associated with slow-delta oscillations on the EEG . We found that after general anesthesia induction with ketamine, the EEG exhibited slow oscillations that alternated with gamma oscillations. The gamma burst pattern has been previously reported during unconsciousness in a visual time-domain description of the pediatric EEG under ketamine (Rosen et al. , 1976). However a neural circuit hypothesis has never been proposed for this finding. The principal glutamatergic arousal pathways emanating from the brainstem are NMDA-mediated glutamatergic projections from the parabrachial nucleus and the medial pontine reticular formation to the thalamus (Saper et al. , 1980, Fulwiler et al. , 1984, Boon et al. , 2008, Fuller et al. , 2011, Kaur et al. , 2013). The parabrachial nucleus also directly sends glutamatergic projections to the basal forebrain (Moga et al. , 1990). Administration of a large-dose of ketamine could lead to disruption of these major glutamatergic excitatory pathways from the parabrachial nucleus and the medial pontine reticular formation to the thalamus and basal forebrain. This would lead to decreased excitatory inputs from the thalamus to the cortex and from the basal forebrain to the cortex, resulting in slow-delta oscillations (Pavone et al. , 2016). Slow-delta oscillations could also be produced by the direct actions of ketamine on the thalamus. Recent rodent experiments have shown that increases in delta power in the frontal cortex induced by NMDA-antagonism have a thalamic source (Kiss et al. , 2011, Zhang et al. , 2012). This does not rule out a loss of brainstem excitation as a mechanism for slow oscillations induced by high-dose ketamine. Rather, it suggests that loss of excitation occurs at afferent synapses in the thalamus, rather than in the brainstem. Other evidence suggests that the thalamus plays an essential role in the generation of ketamine-induced slow oscillation. The gamma burst pattern has been described in cat neurophysiological studies (Miyasaka et al. , 1968, Kayama et al. , 1972). In the intact cat, ketamine induced this oscillatory dynamic in the neocortex, thalamus, caudate nucleus, hippocampus, and brain stem (Miyasaka et al. , 1968, Kayama et al. , 1972).

Together, these previous studies suggest that ketamine could act by blocking NMDA inputs emanating from the brainstem to the thalamus.

Maksimow et al. studied the EEG under ketamine-induced general-anesthesia by maintaining an infusion of S-ketamine in healthy human volunteers (Maksimow et al. , 2006). The authors reported a phenomenon of fast gamma spindles in all subjects during general anesthesia (Maksimow et al. , 2006). It is likely that the fast gamma spindles and the gamma burst pattern we report in this manuscript are the same neurophysiological phenomenon. The transition from the gamma burst pattern to the beta/gamma stable pattern that we report is likely due to decreasing plasma levels of ketamine after the single induction bolus we administered. Thus, repeated boluses of ketamine will induce these slow oscillations (Schwartz et al. , 1974), or an infusion of ketamine at general anesthetic levels will maintain these slow oscillations (Rosen et al. , 1976, Maksimow et al. , 2006). The slow oscillations observed during gamma burst and those that have been described for GABAergic general anesthetic agents may result from different neural circuit mechanisms, and thus they may exhibit different spatiotemporal distribution, and functional characteristics (Mori et al. , 1971).

Ketamine-Induced Gamma, Theta, and Decreased Beta Oscillations

Identifying the roles and physiological significance of gamma (30 – 500 Hz) oscillations in neural information flow is a challenge (Buzsaki et al. , 2015). Ketamine induced gamma oscillations likely result from the ability of ketamine to more effectively block NMDA receptors on fast spiking interneurons than the same receptors on pyramidal neurons (Homayoun et al. , 2007, Seamans, 2008). By selectively down-regulating inhibitory gamma amino-butyric acid (GABA) input to the pyramidal neurons, ketamine disinhibits the pyramidal neurons (Homayoun et al. , 2007, Seamans, 2008). The post-synaptic currents of disinhibited pyramidal neurons likely produce gamma oscillations that are readily observed on the scalp EEG (Homayoun et al. , 2007, Seamans, 2008). Neurochemically, this state is associated with increased cholinergic tone (Kikuchi et al. , 1997, Pal et al. , 2015). Thus, in humans, ketamine-induced gamma oscillations (<50 Hz), which manifest during unconsciousness likely exhibit markedly different frequency, spatiotemporal, and functional characteristics than gamma (>50 Hz) oscillations during normal conscious processing. We found that although the gamma oscillations during gamma burst and beta/gamma stable patterns exhibited differences in the power spectra, their coherence profile was similar. The coherent gamma oscillations could reflect altered neuronal activity that is constrained to particular frequency bands, disrupting cortical information processing and producing a dissociative or amnestic brain-state.

We found that ketamine-induced unconsciousness was also associated with coherent theta oscillations. In adults, theta oscillations have been shown to appear in the absence of gamma oscillations at the lower doses of ketamine used for analgesia and for the treatment of depression (Kochs et al. , 1996, Muthukumaraswamy et al. , 2015). Thus, this oscillatory dynamic may not be sufficient to produce ketamine-induced unconsciousness. Similar to previous reports, we also found that ketamine caused a reduction in alpha-beta oscillations (Corssen et al. , 1966, Engelhardt et al. , 1994, Kochs et al. , 1996, Blain-Moraes et al. ,

2014). Since the decline in alpha-beta oscillation power is associated with analgesic doses of ketamine (Kochs et al. , 1996), and is more prominent at lower ketamine concentrations in our data, this oscillatory dynamic is unlikely by itself to explain ketamine-induced unconsciousness.

Limitations

This is a retrospective report analyzing frontal EEG data. Therefore, our observations should be further studied in prospective high-density EEG investigations. Such investigations will enable spatiotemporal and source space analysis of the EEG signatures we describe in this manuscript, and help relate them to behavioral characterizations of altered consciousness. This will eliminate confounds such as volume conduction which is encountered in studies such as ours, when EEG data analysis is performed in the sensor space. Also, functional characteristics (i.e. phase-phase coupling, phase-frequency coupling) of the EEG signatures during the beta-beta/gamma stable period can be further related to the level of consciousness. These characteristics may enable us to better characterize both arousable and unarousable states of unresponsiveness associated with conscious experiences (i.e. hallucinatory state). Also, intracortical recordings in animal models that closely approximate those obtained in human studies are necessary to better understand the neural circuit mechanisms of these oscillations.

Conclusions

In summary, slow-delta, coherent theta, and coherent gamma oscillations are evident during ketamine-induced brain states. However, ketamine-induced unconsciousness is associated with a characteristic gamma burst pattern in which coherent gamma oscillations alternate with periods of slow oscillations. Presently, pharmacokinetic and pharmacodynamics PK/PD) principles guide all anesthesia drug dosing. Although PK/PD models are regarded to be deterministic and highly accurate in research models, in reality there can be significant patient-to-patient variability in the accuracy and applicability to clinical practice of such models. In the future, we hope that neurophysiological principles such as those described in this manuscript will be incorporated into drug-dosing models and guidelines to enable individualized care. This work also suggests future studies in humans and animal models to characterize the relationships between ketamine-induced states of altered consciousness, brain oscillations, and neural circuit activity. Such studies could lead to an improved understanding of ketamine's anesthetic and anti-depressant properties, and could lead to improved therapies in anesthesia, pain medicine, and psychiatry.

Acknowledgments

Funding

DP2-OD006454 (to PLP); DP1-OD003646, TR01-GM104948 (to ENB), and Ruth L. Kirchstein National Research Service Award to (AH) from the National Institutes of Health, Bethesda, Maryland; Foundation of Anesthesia Education and Research, Rochester, Minnesota (to OA); Massachusetts General Hospital Faculty Development Award, Boston, MA (to OA); Funds from the Department of Anesthesia, Critical Care and Pain Medicine, Massachusetts General Hospital, Boston, MA.

References

Akeju O, Pavone KJ, Thum JA, Firth PG, Westover MB, Puglia M, et al. Age-dependency of sevoflurane-induced electroencephalogram dynamics in children. Br J Anaesth. 2015; 115(Suppl 1):i66–i76. [PubMed: 26174303]

Akeju O, Westover MB, Pavone KJ, Sampson AL, Hartnack KE, Brown EN, et al. Effects of sevoflurane and propofol on frontal electroencephalogram power and coherence. Anesthesiology. 2014; 121:990–8. [PubMed: 25233374]

Arbous MS, Meursing AE, van Kleef JW, de Lange JJ, Spoormans HH, Touw P, et al. Impact of anesthesia management characteristics on severe morbidity and mortality. Anesthesiology. 2005; 102:257–68. quiz 491-2. [PubMed: 15681938]

Blain-Moraes S, Lee U, Ku S, Noh G, Mashour GA. Electroencephalographic effects of ketamine on power, cross-frequency coupling, and connectivity in the alpha bandwidth. Front Syst Neurosci. 2014; 8:114. [PubMed: 25071473]

Boon JA, Milsom WK. NMDA receptor-mediated processes in the Parabrachial/Kolliker fuse complex influence respiratory responses directly and indirectly via changes in cortical activation state. Respir Physiol Neurobiol. 2008; 162:63–72. [PubMed: 18499538]

Buzsaki G, Schomburg EW. What does gamma coherence tell us about inter-regional neural communication? Nat Neurosci. 2015; 18:484–9. [PubMed: 25706474]

Corssen G, Domino EF. Dissociative anesthesia: further pharmacologic studies and first clinical experience with the phencyclidine derivative CI-581. Anesth Analg. 1966; 45:29–40. [PubMed: 5325977]

Cottrell JE. We care, therefore we are: anesthesia-related morbidity and mortality: the 46th Rovenstine Lecture. Anesthesiology. 2008; 109:377–88. [PubMed: 18719435]

Domino EF, Chodoff P, Corssen G. Pharmacologic Effects of Ci-581, a New Dissociative Anesthetic, in Man. Clin Pharmacol Ther. 1965; 6:279–91. [PubMed: 14296024]

Engelhardt W, Stahl K, Marouche A, Hartung E, Dierks T. [Ketamine racemate versus S-(+)-ketamine with or without antagonism with physostigmine. A quantitative EEG study on volunteers]. Anaesthesist. 1994; 43(Suppl 2):S76–82. [PubMed: 7840418]

Ferrer-Allado T, Brechner VL, Dymond A, Cozen H, Crandall P. Ketamine-induced electroconvulsive phenomena in the human limbic and thalamic regions. Anesthesiology. 1973; 38:333–44. [PubMed: 4707578]

Fuller PM, Sherman D, Pedersen NP, Saper CB, Lu J. Reassessment of the structural basis of the ascending arousal system. J Comp Neurol. 2011; 519:933–56. [PubMed: 21280045]

Fulwiler CE, Saper CB. Subnuclear organization of the efferent connections of the parabrachial nucleus in the rat. Brain Res. 1984; 319:229–59. [PubMed: 6478256]

Hering W, Geisslinger G, Kamp HD, Dinkel M, Tschaikowsky K, Rugheimer E, et al. Changes in the EEG power spectrum after midazolam anaesthesia combined with racemic or S- (+) ketamine. Acta Anaesthesiol Scand. 1994; 38:719–23. [PubMed: 7839784]

Homayoun H, Moghaddam B. NMDA receptor hypofunction produces opposite effects on prefrontal cortex interneurons and pyramidal neurons. J Neurosci. 2007; 27:11496–500. [PubMed: 17959792]

Insel TR. Rethinking schizophrenia. Nature. 2010; 468:187–93. [PubMed: 21068826]

Kaur S, Pedersen NP, Yokota S, Hur EE, Fuller PM, Lazarus M, et al. Glutamatergic signaling from the parabrachial nucleus plays a critical role in hypercapnic arousal. J Neurosci. 2013; 33:7627–40. [PubMed: 23637157]

Kayama Y, Iwama K. The EEG, evoked potentials, and single-unit activity during ketamine anesthesia in cats. Anesthesiology. 1972; 36:316–28. [PubMed: 5020641]

Kikuchi T, Wang Y, Shinbori H, Sato K, Okumura F. Effects of ketamine and pentobarbitone on acetylcholine release from the rat frontal cortex in vivo. Br J Anaesth. 1997; 79:128–30. [PubMed: 9301402]

Kiss T, Hoffmann WE, Scott L, Kawabe TT, Milici AJ, Nilsen EA, et al. Role of Thalamic Projection in NMDA Receptor-Induced Disruption of Cortical Slow Oscillation and Short-Term Plasticity. Front Psychiatry. 2011; 2:14. [PubMed: 21556284]

Kochs E, Scharein E, Mollenberg O, Bromm B, Schulte am Esch J. Analgesic efficacy of low-dose ketamine. Somatosensory-evoked responses in relation to subjective pain ratings. Anesthesiology. 1996; 85:304–14. [PubMed: 8712446]

Langsjo JW, Maksimow A, Salmi E, Kaisti K, Aalto S, Oikonen V, et al. S-ketamine anesthesia increases cerebral blood flow in excess of the metabolic needs in humans. Anesthesiology. 2005; 103:258–68. [PubMed: 16052107]

Langsjo JW, Salmi E, Kaisti KK, Aalto S, Hinkka S, Aantaa R, et al. Effects of subanesthetic ketamine on regional cerebral glucose metabolism in humans. Anesthesiology. 2004; 100:1065–71. [PubMed: 15114201]

Lee U, Ku S, Noh G, Baek S, Choi B, Mashour GA. Disruption of frontal-parietal communication by ketamine, propofol, and sevoflurane. Anesthesiology. 2013; 118:1264–75. [PubMed: 23695090]

Maksimow A, Sarkela M, Langsjo JW, Salmi E, Kaisti KK, Yli-Hankala A, et al. Increase in high frequency EEG activity explains the poor performance of EEG spectral entropy monitor during S-ketamine anesthesia. Clin Neurophysiol. 2006; 117:1660–8. [PubMed: 16807101]

Miyasaka M, Domino EF. Neural mechanisms of ketamine-induced anesthesia. Int J Neuropharmacol. 1968; 7:557–73. [PubMed: 5753175]

Moga MM, Herbert H, Hurley KM, Yasui Y, Gray TS, Saper CB. Organization of cortical, basal forebrain, and hypothalamic afferents to the parabrachial nucleus in the rat. J Comp Neurol. 1990; 295:624–61. [PubMed: 1694187]

Mori K, Kawamata M, Mitani H, Yamazaki Y, Fujita M. A neurophysiologic study of ketamine anesthesia in the cat. Anesthesiology. 1971; 35:373–83. [PubMed: 4329802]

Muthukumaraswamy SD, Shaw AD, Jackson LE, Hall J, Moran R, Saxena N. Evidence that Subanesthetic Doses of Ketamine Cause Sustained Disruptions of NMDA and AMPA-Mediated Frontoparietal Connectivity in Humans. J Neurosci. 2015; 35:11694–706. [PubMed: 26290246]

Pal D, Hambrecht-Wiedbusch VS, Silverstein BH, Mashour GA. Electroencephalographic coherence and cortical acetylcholine during ketamine-induced unconsciousness. Br J Anaesth. 2015; 114:979–89. [PubMed: 25951831]

Pavone KJ, Akeju O, Sampson AL, Ling K, Purdon PL, Brown EN. Nitrous oxide-induced slow and delta oscillations. Clin Neurophysiol. 2016; 127:556–64. [PubMed: 26118489]

Percival, DB.; Walden, AT. Multitaper Spectral Estimation. Spectral Analysis for Physical Applications. Cambridge University Press; Cambridge, United Kingdom: 1993.

Purdon PL, Pavone KJ, Akeju O, Smith AC, Sampson AL, Lee J, et al. The Ageing Brain: Age-dependent changes in the electroencephalogram during propofol and sevoflurane general anaesthesia. Br J Anaesth. 2015a; 115(Suppl 1):i46–i57. [PubMed: 26174300]

Purdon PL, Sampson A, Pavone KJ, Brown EN. Clinical Electroencephalography for Anesthesiologists: Part I: Background and Basic Signatures. Anesthesiology. 2015b; 123:937–60. [PubMed: 26275092]

Rosen I, Hagerdal M. Electroencephalographic study of children during ketamine anesthesia. Acta Anaesthesiol Scand. 1976; 20:32–9. [PubMed: 1266554]

Saper CB, Loewy AD. Efferent connections of the parabrachial nucleus in the rat. Brain Res. 1980; 197:291–317. [PubMed: 7407557]

Schultz A, Schultz B, Zachen B, Pichlmayr I. The effects of ketamine on the electroencephalogram--typical patterns and spectral representations. [Article in German]. Anaesthesist. 1990; 39:222–5. [PubMed: 2339774]

Schwartz MS, Virden S, Scott DF. Effects of ketamine on the electroencephalograph. Anaesthesia. 1974; 29:135–40. [PubMed: 4819066]

Seamans J. Losing inhibition with ketamine. Nat Chem Biol. 2008; 4:91–3. [PubMed: 18202677]

Vuyk, J.; Sitsen, E.; Reekers, M. Intravenous Anesthetics.. In: Miller, RD., editor. Miller's Anesthesia. Eighth ed.. Elsevier/Saunders; Philadelphia, PA: 2015.

White PF, Schuttler J, Shafer A, Stanski DR, Horai Y, Trevor AJ. Comparative pharmacology of the ketamine isomers. Studies in volunteers. Br J Anaesth. 1985; 57:197–203. [PubMed: 3970799]

Zarate CA Jr. Singh JB, Carlson PJ, Brutsche NE, Ameli R, Luckenbaugh DA, et al. A randomized trial of an N-methyl-D-aspartate antagonist in treatment-resistant major depression. Arch Gen Psychiatry. 2006; 63:856–64. [PubMed: 16894061]

Zhang Y, Yoshida T, Katz DB, Lisman JE. NMDAR antagonist action in thalamus imposes delta oscillations on the hippocampus. J Neurophysiol. 2012; 107:3181–9. [PubMed: 22423006]

Highlights

- Slow-delta oscillations that alternate with gamma oscillations (gamma burst) occur with ketamine at general anesthesia levels.
- Gamma, theta and decreased alpha/beta oscillations are not unique to ketamine at general anesthesia levels.
- The gamma burst pattern may result from circuit disruptions in cortical and subcortical sites.

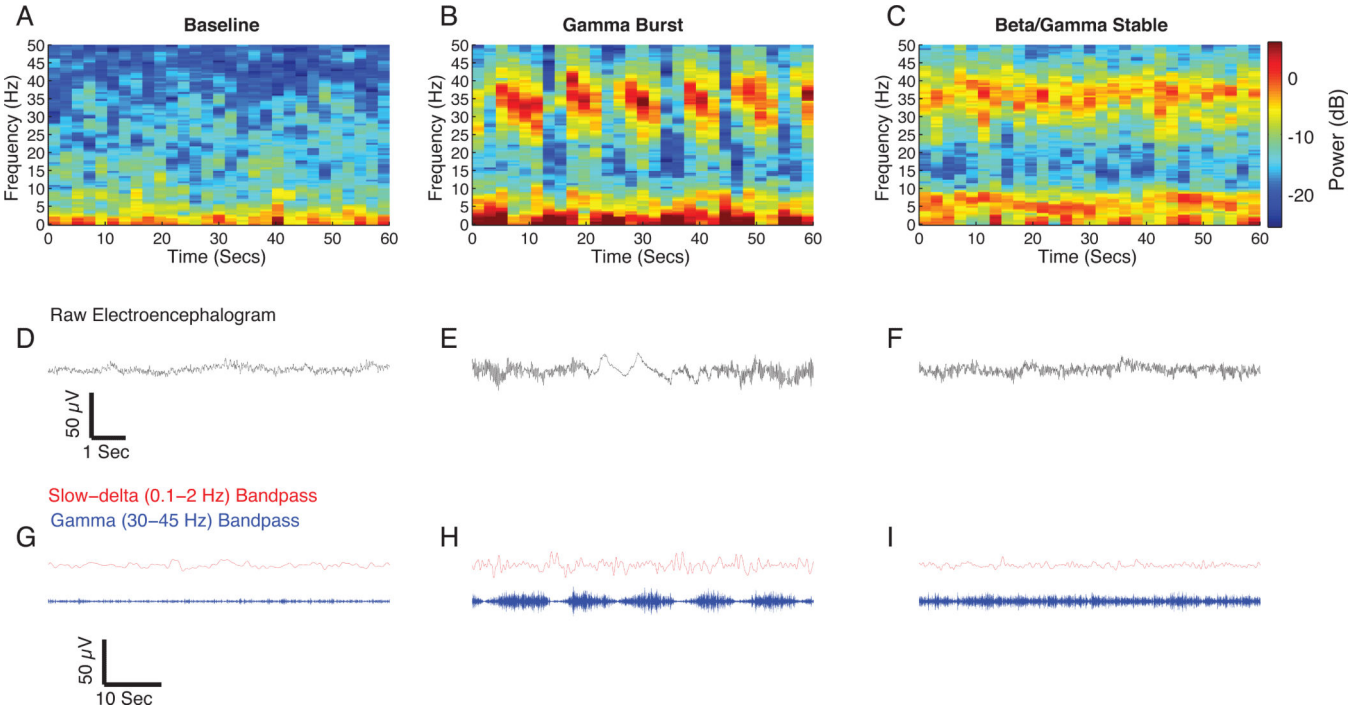

Figure 1.

Representative spectrogram and time-domain traces of baseline and ketamine-induced EEG signatures. A. Baseline spectrogram with a relative lack of power concentrated in any frequency band. B. Gamma burst spectrogram with power concentrated in slow-delta, theta, and gamma frequency bands. The increased gamma power can be observed to occur in a rhythmic pattern that alternates with slow-delta oscillations. C. Beta/gamma stable spectrogram with power concentrated in theta and gamma frequency bands. The gamma pattern does not demonstrate an appreciable rhythmicity. D. Representative 10 second raw EEG trace from panel A. E. Representative10 second raw EEG trace from panel B illustrating the alternating slow-delta oscillation and gamma oscillation pattern. F. Representative10 second raw EEG trace from panel C illustrating the stable gamma pattern. G. Representative 55 second slow (red) and gamma (blue) band passed filtered EEG trace from panel A. H. Representative 55 second slow and gamma band passed filtered EEG trace from panel B. Compared to baseline, the gamma burst pattern is visually evident. I. Representative 55 second slow (red) and gamma (blue) band passed filtered EEG trace from panel C. Compared to gamma burst, the gamma pattern is not rhythmic.

dB = decibel; Hz = hertz.

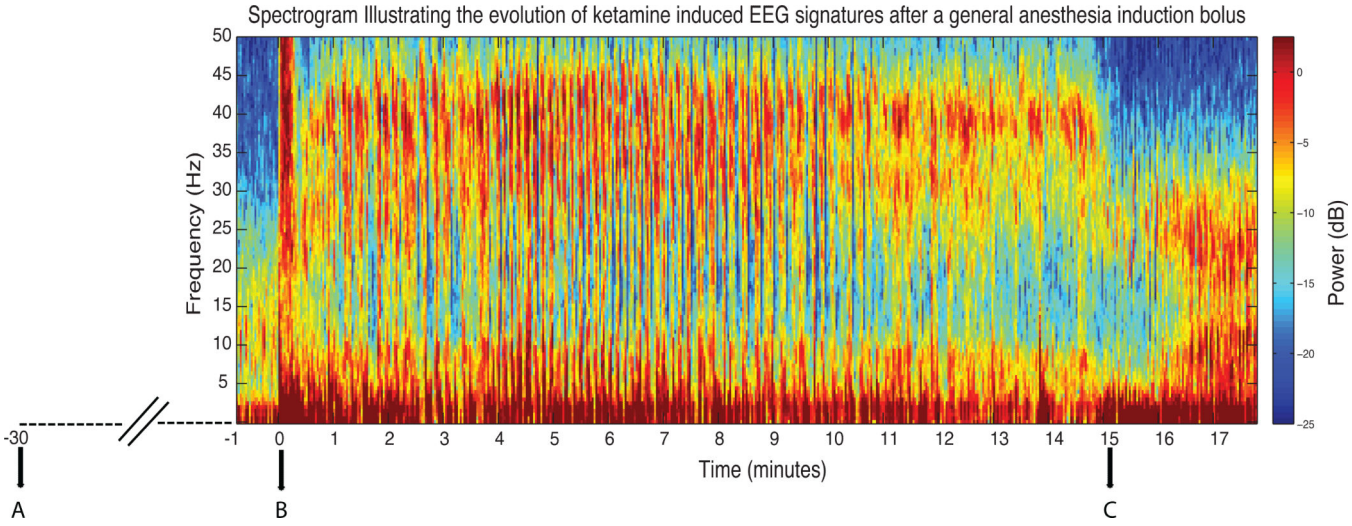

Figure 2.

Illustrative spectrogram showing the evolution of ketamine induced electroencephalogram signatures after a general anesthesia induction bolus. At time point A, 2 mg of midazolam and 100mcg of fentanyl was administered. At time point B, 200 mg of ketamine was administered to induce general anesthesia. Muscle artifact (solid red band encompassing 0-50 Hz) can be noted at this time point. Between time-points B and C, the gamma burst and the beta/gamma patterns can both be observed. At time point C, the anesthetic vapor isoflurane was administered to maintain surgical unconsciousness. Upon the administration of isoflurane, the beta/gamma pattern transitions into an EEG pattern encountered when modern day derivatives of ether (desflurane, isoflurane, sevoflurane) are administered concurrently with ketamine (markedly increased slow, delta, theta, and alpha/beta power). dB = decibel; EEG = electroencephalogram; Hz = hertz.

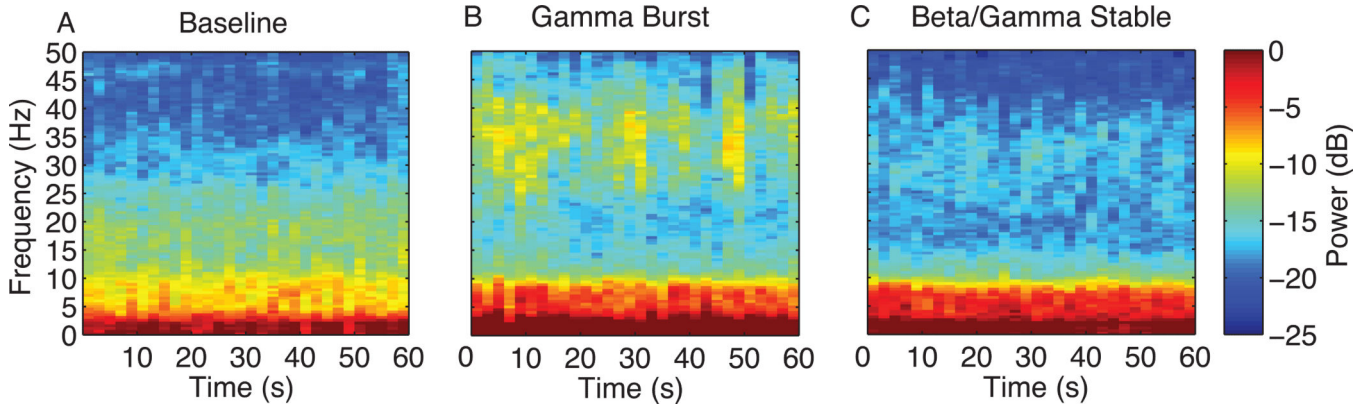

Figure 3.

Group-level spectrograms within the 0 to 50 Hz frequency range computed from 1 minute segments prior to surgical stimulation. A. Median spectrogram during baseline showing a relative absence of power in the theta and gamma frequency bands and power in the alpha/beta frequency band (n = 12). B. Median spectrogram during gamma burst. Compared to baseline, there is increased power in the slow, theta and gamma frequency bands and decreased power in the alpha/beta frequency band. C. Median spectrogram during beta/gamma stable. Compared to baseline, there is increased power in the theta and gamma frequency bands and decreased power in the alpha/beta frequency band (n = 11).
dB = decibel; Hz = hertz.

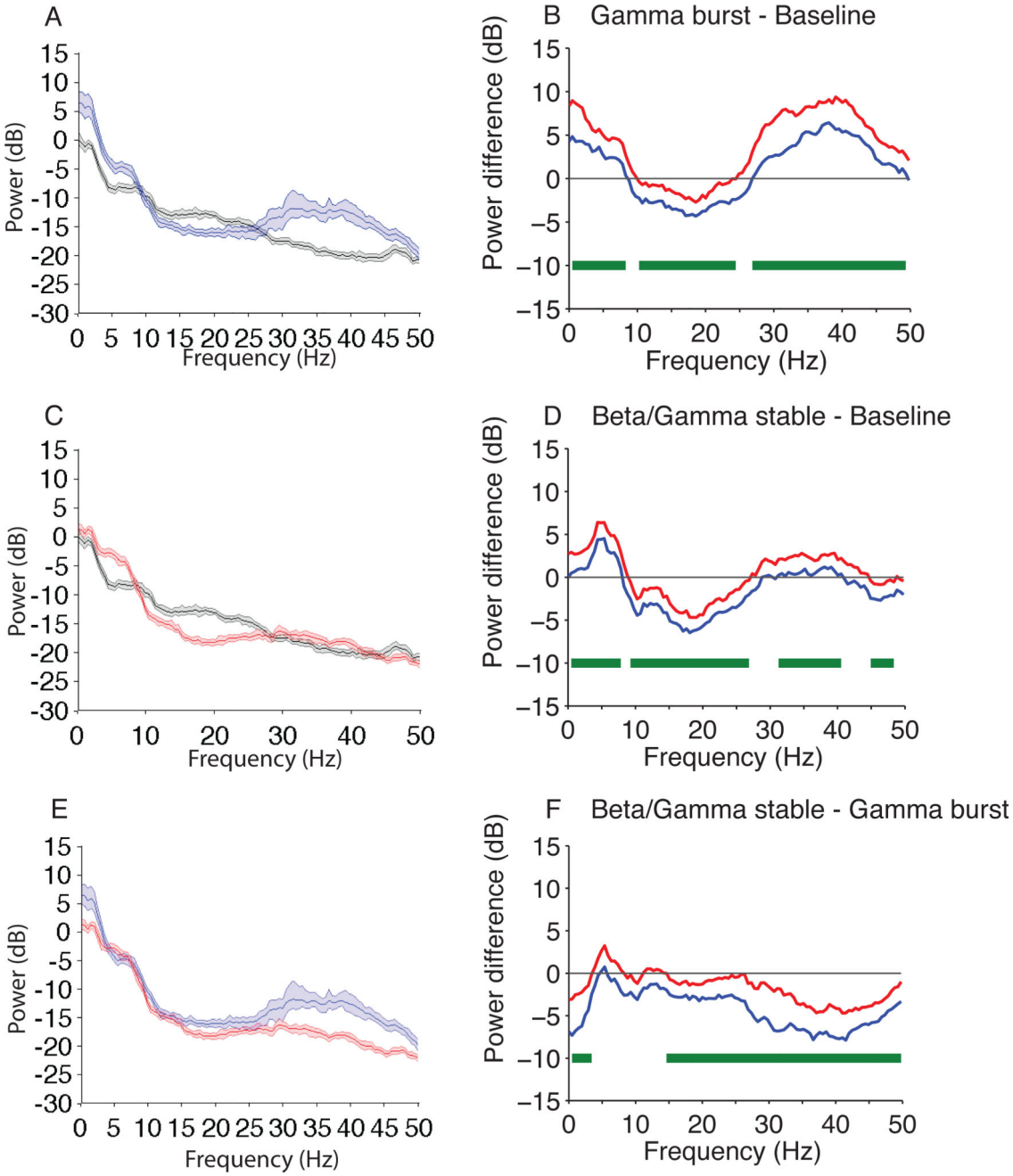

Figure 4.

Group-level spectral analyses comparing baseline, gamma burst, and beta/gamma stable. (A). Power spectra of baseline (black) *versus* gamma burst (blue). Bootstrapped median spectra are presented and the shaded regions represent the 95% confidence interval for the uncertainty around each median spectrum. (B) The upper (red) and lower (blue) represent the bootstrapped 95% confidence interval bounds for the difference between spectra shown in panel A. EEG power was significantly larger than baseline at 0.1-8.3 Hz and 26.9-50 Hz, and smaller than baseline at 10.3-24.4 Hz. (C). Power spectra of baseline (black) *versus* beta/gamma stable (red). Bootstrapped median spectra are presented and the shaded regions

represent the 95% confidence interval for the uncertainty around each median spectrum. (D) The upper (red) and lower (blue) represent the bootstrapped 95% confidence interval bounds for the difference between spectra shown in panel C. EEG power was significantly larger than baseline at 0.1-7.8 Hz and 31.25-40 Hz, and smaller than baseline at 9.2-26.9 Hz and 44.9-48.3 Hz. (E). Power spectra of gamma burst *versus* beta/gamma stable. Bootstrapped median spectra are presented and the shaded regions represent the 95% confidence interval for the uncertainty around each median spectrum. (F) The upper (red) and lower (blue) represent the bootstrapped 95% confidence interval bounds for the difference between spectra shown in panel E. EEG power was significantly larger than beta/gamma stable at 0.1-3.4 Hz, and 16.1-50 Hz.

Horizontal solid green lines represents frequency ranges at which significant difference existed. dB = decibel; Hz = hertz.

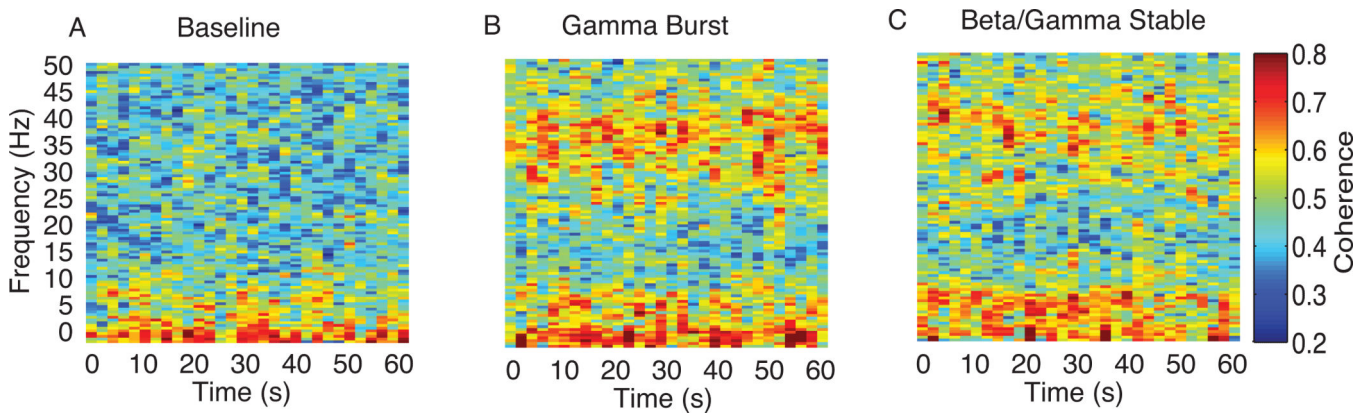

Figure 5.

Group-level Coherograms within the 0 to 50 Hz frequency range computed from 1-minute segments prior to surgical stimulation. A. Median coherogram during baseline showing a relative absence of coherence in theta, alpha, beta and gamma frequency bands (n = 12). B. Median coherogram during gamma burst. Compared to baseline, there is increased coherence in slow, delta, theta, and gamma frequency bands (n = 12). C. Median coherogram during beta/gamma stable. Compared to baseline, there is increased coherence in theta and gamma frequency bands (n = 11).

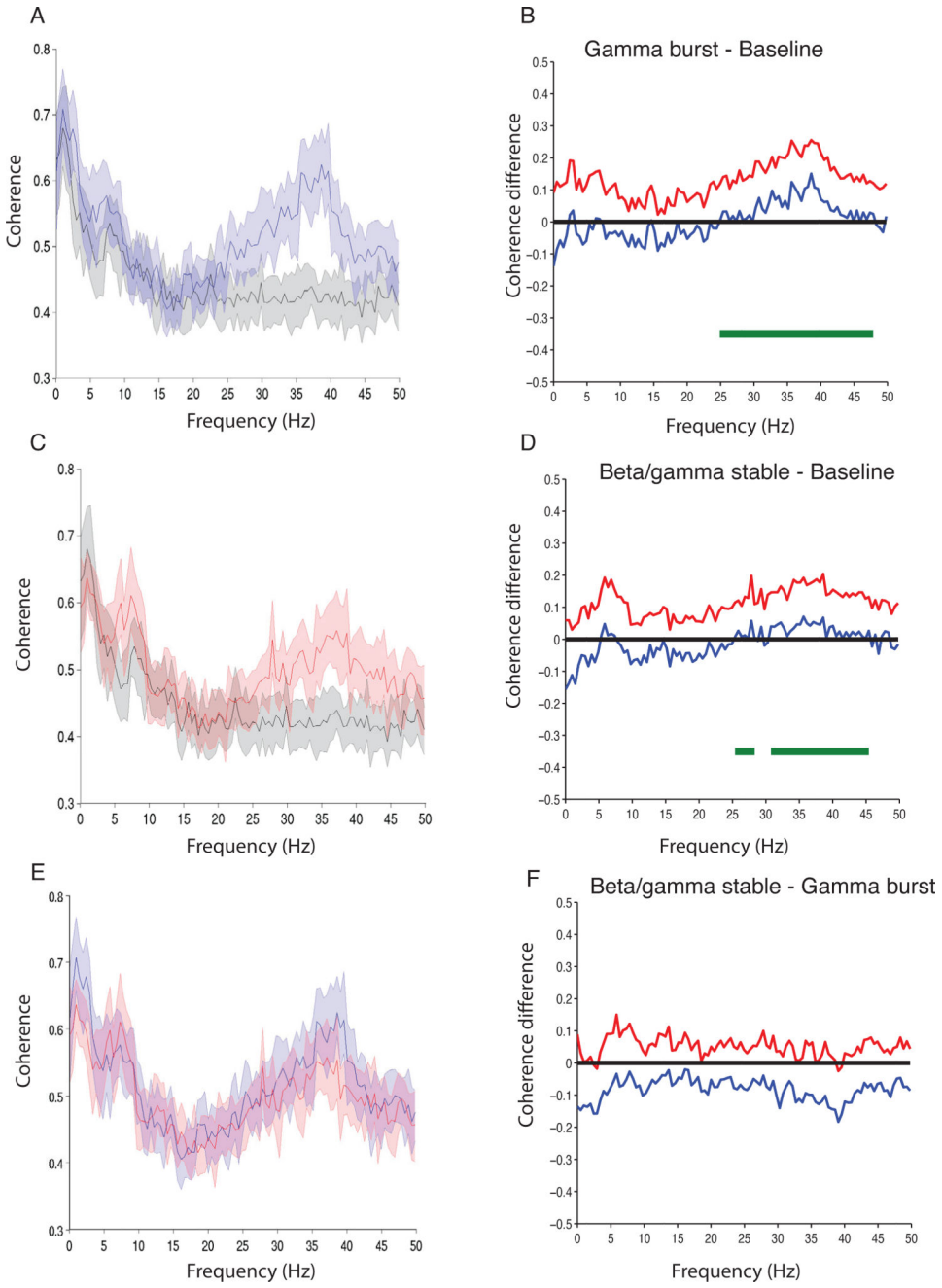

Figure 6.

Group-level coherence analyses comparing baseline, gamma burst, and beta/gamma stable. (A). Coherence analysis of baseline (black) *versus* gamma burst (blue). Bootstrapped median coherences are presented and the shaded regions represent the 95% confidence interval for the uncertainty around the median coherence. (B) EEG was significantly more coherent than baseline at 27.9-48.9 Hz).. The upper (red) and lower (blue) represent the bootstrapped 95% confidence interval bounds for the difference between coherence shown in panel A (C). Coherence analysis of baseline (black) *versus* beta/gamma stable (red). Bootstrapped median coherences are presented and the shaded regions represent the 95%

confidence interval for the uncertainty around each median coherence. (D) EEG was significantly more coherent than baseline at 25.4–28.3 and 30.8–45.5 Hz. The upper (red) and lower (blue) represent the bootstrapped 95% confidence interval bounds for the difference between coherence shown in panel C. (E). Coherence analysis of gamma burst (blue) *versus* beta/gamma stable (red). Bootstrapped median coherences are presented and the shaded regions represent the 95% confidence interval for the uncertainty around teach median coherence. (F) EEG coherence was similar between both groups, even though gamma burst (blue) appeared to exhibit a larger slow-delta coherence. The upper (red) and lower (blue) represent the bootstrapped 95% confidence interval bounds for the difference between coherence shown in panel E.

Horizontal solid green lines represent frequency ranges at which significant difference existed. dB = decibel; Hz = hertz.

Table 1

Patient characteristics and co-administered medications.

	Age	Sex	Weight (kg)	Midazolam (mg)	Fentanyl (mcg)	Ketamine Induction Dose (mg/kg)	Gamma Burst at LOC	Gamma Burst Duration (secs)	Nerve Block	Neuromuscular blocker
Patient A	28	M	81.8	*2	*100	2	✓	321	✓	✓
Patient B	38	M	102	2	250	2	✓	333	✗	✓
Patient C	40	F	55	-	-	2.2	✓	528	✗	✓
Patient D	48	M	91	-	-	2.2	✓	355	✗	✓
Patient E	55	M	88.64	*2	*100	2.3	✓	224	✗	✓
Patient F	53	M	70	-	250	2.9	✓	**	✗	✓
Patient G	57	F	59	0.5	100	2	✓	299	✗	✓
Patient H	57	M	62	*2	*100	3.2	✓	472	✓	✓
Patient I	60	M	103	2	250	1.9	✓	262	✗	✓
Patient J	60	M	91	2	-	2.2	✓	366	✗	✓
Patient K	62	M	77	-	250	1.9	✓	345	✗	✓
Patient L	63	M	82	2	250	2	✓	160	✗	✓
Mean (±SD)			80.2 (16.1)	1.8 (0.5)	183 (79)	2.2 (0.4)		333.3 (103.5)		
n (%)							12 (100)		2 (17)	12 (100)

SD, standard deviation

*Drug was administered > 30 minutes prior to the induction of general anesthesia

**Anesthetic vapor was administered prior to the transition of the gamma burst to the beta/gamma stable pattern. The gamma/stable pattern occurred in all other patients.